 DOI: 10.1002/masy.200750218

RAFT Polymerization in Bulk and Emulsion

Alessandro Buttè, A. David Peklak, Giuseppe Storti, Massimo Morbidelli

Summary: Detailed models of the RAFT polymerization in both non-segregated (bulk) and segregated (seeded emulsion) systems are presented. It is shown that satisfactory agreements between experiments and models can be achieved, and that effects such as inhibition and retardation, or the polymerization behavior at high conversions can be readily explained. In all cases the model parameter fitting has been minimized, being mostly limited to the rate coefficients of the addition/fragmentation reactions in the RAFT polymerization. Therefore, such models are believed to be invaluable tools towards a deeper understanding of the main phenomena underlying RAFT polymerization.

Introduction

Among the different techniques presented in the literature to carry out a living free-radical polymerization (LRP), reversible addition–fragmentation chain transfer (RAFT) polymerization has attracted particular attention.[1] Two main reasons can be identified for its success: (1) the large versatility of the process and (2) its peculiar chemistry. The latter is illustrated in Figure 1: a polymer chain capped e.g. by a dithiocarbonyl group (RAFT group), also called a dormant chain, D_m, and a radical chain, $R_n^\bullet$, undergo first an addition reaction to form an intermediate radical, $T_{n,m}^\bullet$, in which both chains are attached to the RAFT group. Because this intermediate radical is unstable, it breaks either giving back the original chains, or resulting in the exchange of the RAFT group between the two chains. Since the rate of fragmentation is typically much faster than that of addition, the RAFT reaction is often approximated as transfer reaction of the RAFT group and it is then supposed not to affect the overall radical concentration. As a consequence, the same kinetics of monomer consumption as in conventional free-radical polymerization processes is expected.

Despite this ideal description, it became soon evident that the true kinetics of RAFT polymerization is more complex. Experimental observations as (i) long inhibition times at the beginning of the reaction,[2] (ii) polymerization rates slower than the corresponding non-living processes (retardation),[3] and (iii) a less pronounced gel effect at high conversion values[4a] have been often reported.

To approach truly living conditions in free radical polymerization, the extent of the termination reactions has to be reduced as much as possible. The natural way to establish such conditions is the reduction of the concentration of active chains, which, in turn, results in the decrease of polymer productivity. To contrast such decrease, the segregation of the radical chains, which is present in heterogeneous processes such as emulsion polymerization, can be exploited. This allows reducing terminations while preserving the overall concentration of radical chains. However, the application of RAFT mediated polymerizations to emulsion systems has also been rather problematic, mainly with respect to the transport of RAFT agent through the aqueous phase. Attempts to carry out RAFT polymerizations in *ab-initio* emulsion processes

Institute for Chemical and Bioengineering, Department of Chemistry and Applied Biosciences, ETH Zurich, 8093 Zurich, Switzerland
E-mail: alessandro.butte@chem.ethz.ch

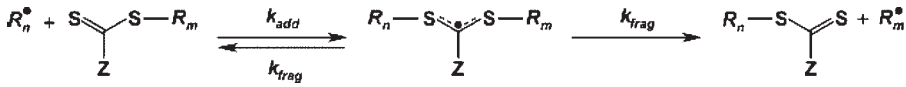

Figure 1.
Schematic representation of the RAFT reaction. $R_n^\bullet$ represents a polymer radical chain; $R_m - S - C(-Z) = S$ a dormant chain (D_m); and $R_m - S - C^\bullet(-Z) - S - R_n$ an intermediate radical ($T_{n,m}^\bullet$).

typically led to the formation of coagulum and to unfeasibly low reaction rates.[5] To overcome such inconveniences, either the transport of the RAFT agent through the aqueous phase has to be enhanced, e.g., through the use of cyclodextrines,[6] or different approaches to establish segregation have to be employed, such as miniemulsion.[7,8] Recently, the successful application of RAFT polymerization to seeded emulsion systems by distributing the RAFT agent in the emulsion seed prior to the actual polymerization with an acetone transport technique has been reported.[9] Experimental results suggest that the kinetics of such polymerizations is significantly different from that of conventional seeded emulsion polymerization. In particular, considerable inhibition times before the onset of monomer consumption, as well as reduced reaction rates (retardation) in comparison to the equivalent nonliving reactions have been observed.

While most of the research activity referred above was focused on the kinetic analysis of the first part of the polymerization, the reaction behavior at high conversion has been investigated much less.[4] Nonetheless, this problem deserves special attention because the chemistry of the RAFT reaction involves a direct reaction of two polymer chains and, therefore, can be strongly affected by diffusion limitations. Wang and Zhu analyzed the effects of diffusion limitations and chain-length dependent rate constants through model calculations.[10] They demonstrated that the polymerization kinetics is controlled by diffusion limitations at high conversions only and that the same limitations slow down the RAFT mechanism, thus making the control of the polymer growth more difficult.

In this work, the previous two issues, namely the behavior of the polymerization at very low and very high conversion values, will be addressed. In the first case, it will be shown that, in spite of the fact that both non-segregated and segregated systems exhibit inhibition and retardation, the cause for these two effects is different in the two systems. In the case of non-segregated systems, this analysis will be supported by a simple analytical solution. The issue of the system behavior at high conversion values will be addressed for non-segregated systems only, since in these systems the change in behavior due to diffusion limitations is most pronounced. In particular, it will be shown that a complete description of the chain length distribution (CLD) is of paramount importance to accurately predict the system behavior.

Inhibition and Retardation in Non-Segregated Systems

A typical kinetic scheme for homogeneous systems is considered, which includes radical initiation (k_i), monomer propagation (k_p), bimolecular termination by radical combination (k_t), and RAFT reaction, i.e., addition reaction to a dormant chain (k_{add}) and fragmentation of the radical intermediate (k_{frag}). In addition, bimolecular termination by combination of radicals with the radical intermediates (k_{it}) has been included. The methodology first proposed by Fischer[11] to study the persistent radical effect in NMLP is used to find an analytical solution for the mass balances on the different species (radicals, $R^\bullet$, intermediate radicals, $T^\bullet$, and dormant chains, D). In particular, by plotting the solution in a log-log scale, it has been shown[12] that it becomes possible to identify distinct time intervals or regions where the different

dimensionless concentrations follow a power law like $c = a\tau^b$, where $c(\tau)$ is the generic dimensionless concentration, while a and b are constants. Moreover, the same balances can be expressed into a non-dimensional form, where the concentration of the radicals ($R^\bullet$ and $T^\bullet$) are made dimensionless using the stationary expression of the radical concentration in non-living bulk polymerization ($R_s^\bullet = \sqrt{R_i/k_t}$), the dormant and dead chains using the initial concentration of dormant chains ($D^{(0)}$), and the time using the process characteristic time $[1/(k_p R_s^\bullet)]$, so to obtain the quantities r, q, d and τ, respectively (cf Figures 2 to 4). As a result, it is possible to identify a set of dimensionless parameters which can be used to predict the polymerization behavior. Among them, the parameter α is of particular importance, defined as follows:

$$\alpha = k_{add} D^{(0)} / k_{frag} \tag{1}$$

This parameter represents the ratio between the frequency at which one radical reacts with a dormant chain and the frequency at which an intermediate radical fragments. Therefore, it is directly related to the accumulation of intermediate radicals. Another relevant quantity is the parameter ε_r, defined as:

$$\varepsilon_r = k_{ti}/k_t \tag{2}$$

Such quantity is the ratio between radical-intermediate and radical-radical termination rate constants.

Let us analyze the system behavior in terms of dimensionless concentrations at different values of such key parameters. In Figure 2, the log-log plot of the dimensionless concentrations of radicals (r) and intermediate radicals (q) versus the non-dimensional reaction time (τ) is shown for the case $\alpha < 1$ and in the absence of intermediate radical termination ($\varepsilon_r = 0$). Looking at the radical concentration, two well-distinct regions can be identified: in the first one, the radical concentration grows with slope one; while in the second one a steady-state value is established. This takes place at dimensional time $t_2 = 1/(k_t R_s^\bullet)$ (corresponding to τ_2 of Figure 1), which corresponds to the characteristic time of the termination reactions. It can be easily proved that such a behavior is equal to that of a non-living polymeriza-

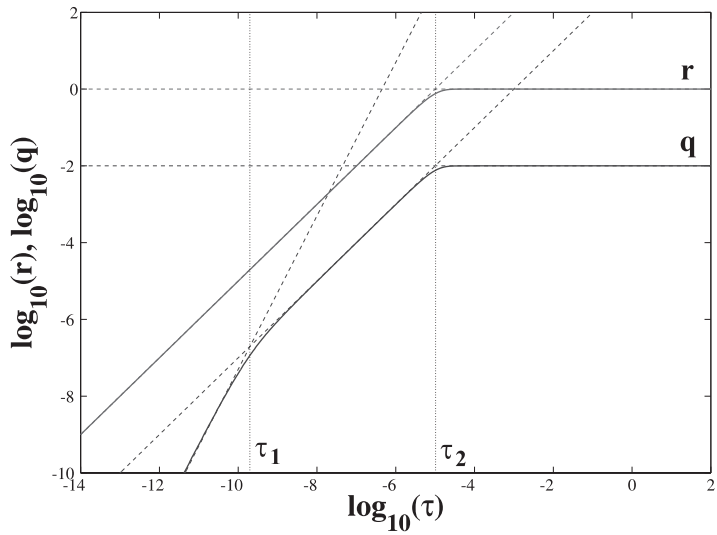

Figure 2.
Logarithmic dimensionless concentration of intermediate radicals (q) and radicals (r) versus non-dimensional polymerization time (τ) for $\alpha = 10^{-2}$ in the absence of intermediate termination ($\varepsilon_r = 0$). More details in Ref. 12, Figure 2.

tion: therefore, the same concentration profile is expected in the two cases at low conversion values. The same analysis can be repeated for the concentration of the intermediate radicals. When large enough concentration of intermediate radicals is built up, the rate of addition equilibrates the rate of fragmentation. The time needed to build up this concentration corresponds to the characteristic time of the fragmentation reaction, $t_1 = 2/k_{frag}$ (corresponding to τ_1 of Figure 1). At this point, the concentration of the intermediates reaches a quasi-steady state (QSS) value and the same QSS concentration is maintained when the radical concentration reaches the steady-state behavior. Note that α represents the steady state concentration of the intermediate radicals.

The case $\alpha > 1$, i.e., the case where the frequency of fragmentation is smaller than that of addition, is shown in Figure 3. The radical concentration, r, is initially growing due to radical initiation as in Figure 2, while the intermediate radicals accumulate due to addition to the dormant chains. At $\tau = \tau_1$, which corresponds to the characteristic time of the addition reaction, the production of new radicals by initiation is equilibrated by the rate of addition [i.e., $k_{add}DR^{\bullet} = R_i$]. This temporary solution is valid as long as the concentration of the intermediates is small enough. At $\tau = \tau_3$, which corresponds to the characteristic time of fragmentation, the production of radicals by fragmentation becomes predominant: fragmentation and addition proceed with the same reaction rate and the radical concentration reaches a QSS value with respect to the intermediate concentration. This situation lasts until both material balances reach the steady-state at $\tau = \tau_4$. By comparison of Figures 2 and 3, it can be noticed that the radical concentration profile follows two different paths depending on the value of α: for $\alpha < 1$, the radical concentration follows the path A-B-C, while for $\alpha > 1$ it follows the path A-D-C. Accordingly, it can be said that the segment AD = BC represents the delay introduced in the reaction due to the slower fragmentation rate. In other words, the inhibition time can be roughly estimated as $t_{inhib} = t_C - t_B \approx t_C = \alpha/(k_t R_s^{\bullet})$. It can be therefore concluded that, in the case of slow fragmentation, an inhibition time is

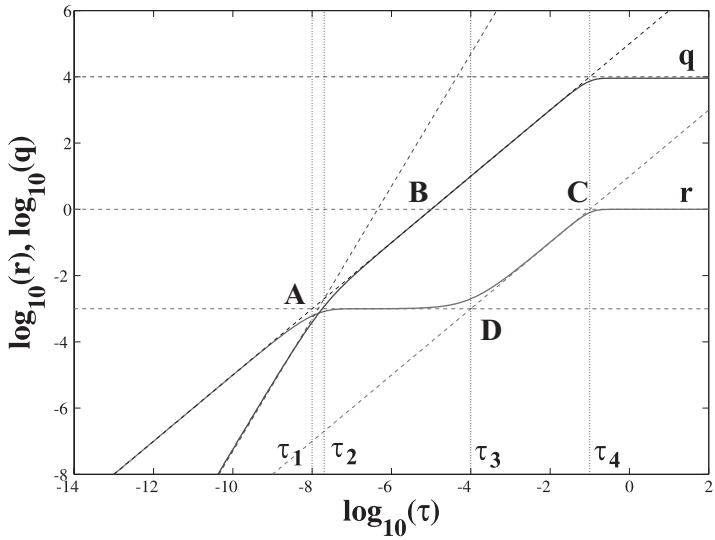

Figure 3.
Logarithmic dimensionless concentration of intermediate radicals (q) and radicals (r) versus non-dimensional polymerization time (τ) for $\alpha = 10^4$ in the absence of intermediate termination ($\varepsilon_r = 0$). More details in Ref. 12, Figure 5.

expected at the beginning of the polymerization. On the other hand, it should be also observed that, since α corresponds to the dimensionless steady state concentration of intermediate radicals, this analysis is valid as long as this value is much smaller than the initial concentration of dormant chains. It can be shown that, as a result, the ratio between the maximum inhibition time and the process time is $t_{inhib}^{max}/t_{proc} = 1/(2\gamma)$, where γ represents the ratio between the dead chains and the dormant chains at the characteristic process time. Accordingly, when the targeted livingness of the process is very large ($\gamma \ll 1$), large inhibition times can be actually observed.

It is now interesting to analyze the latter case in the presence of the intermediate termination ($0 < \varepsilon_r < 1$). This is shown in Figure 4, where again the radical concentrations are plotted versus the dimensionless time. An additional plateau appeared in the evolution of the radical concentration, r, at time $\tau = \tau_3$, while for shorter times the solution is identical to that in Figure 3. At $\tau = \tau_3$, an equilibrium is reached between the rates of radical initiation and bimolecular termination. However, due to the simultaneous termination of the radicals with the intermediate radicals, the overall rate of termination is larger compared to the cases in Figure 2 and 3 and, thus, a smaller QSS value is reached. On the other hand, every time an intermediate radical is consumed, a RAFT agent is subtracted from the activation/deactivation equilibrium. This leads to a faster consumption of the RAFT agent, so that, at $\tau = \tau_4$, no more dormant chains are available in the system and the reaction continues as a non-living one. As a side effect, the value of r reaches its final steady-state, since the intermediate termination rate also drops to zero. Accordingly, in the presence of intermediate termination, a lower steady state value of the radical concentration is achieved [$r^2 = 1/(1 + 2\alpha\varepsilon_r d)$], thus explaining the occurrence of retardation in some experimental observations. It should be noted that recently a different intermediate termination mechanism has been proposed, which not involved the consumption of the RAFT agent.[13] In this case, the analysis remains valid up to the final decay in the dormant chain concentration.

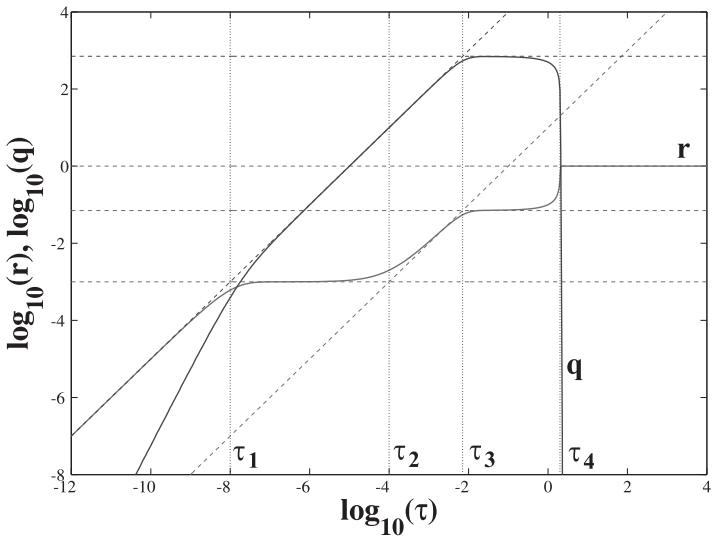

Figure 4.
Logarithmic dimensionless concentration of intermediate radicals (q) and radicals (r) versus non-dimensional polymerization time (τ) for $\alpha = 10^4$ in the presence of intermediate termination ($\varepsilon_r = 10^{-2}$). More details in Ref. 12, Figure 8.

Inhibition and Retardation in Segregated Systems

Living seeded emulsion polymerizations, using cumyl dithiobenzoate as RAFT agent, were performed at different levels of initiator and RAFT agent, as shown in Figure 5.[14] With respect to the central experiment, having an initial RAFT agent concentration equal to 8.41 mM and an initiator concentration of 1.7 mM, two more sets of experiments have been carried out to check the sensitivity on conversion to both RAFT agent and initiator concentration. It can be noticed that both inhibition time and slope of the conversion curve depend on the initiator as well as on the RAFT agent concentration. Whereas an increase of initiator concentration promotes larger reaction rates and shorter inhibition times, the opposite is true for the RAFT agent concentration: here, an increase leads to increased inhibition time and decreased reaction rate. Notably, the reaction rate is much more sensitive to RAFT agent than to initiator concentration.

To understand the changes in inhibition time and retardation, it is useful to analyze in detail the model results of the central experiment (Run 3 of Table 1) at two times during the reaction: (i) at the very beginning, when the polymerization rate is extremely small, so as to investigate the inhibition, and (ii) at the time where steady state is reached, so as to investigate the retardation. Figure 6 visualizes the situation at the beginning of the polymerization. The absorption of a short radical in N_0 particles (with frequency a) changes the particle state to N_1(short), where this notation indicates a particle with one ''short'' radical, i.e. a radical able to desorb. In the N_1(short) population, desorption dominates over all other mechanisms. However, the radical can also propagate and this changes the particle state to N_1(long), i.e. a radical which cannot desorb is formed. In this state, RAFT exchange with the RAFT agent dominates and leads to the formation of a RAFT leaving group radical. This brings the particle state back to N_1(short), since the RAFT leaving group is typically short and can be easily extracted by the aqueous phase. Since in N_1(short) the most likely fate of this radical is desorption, it can

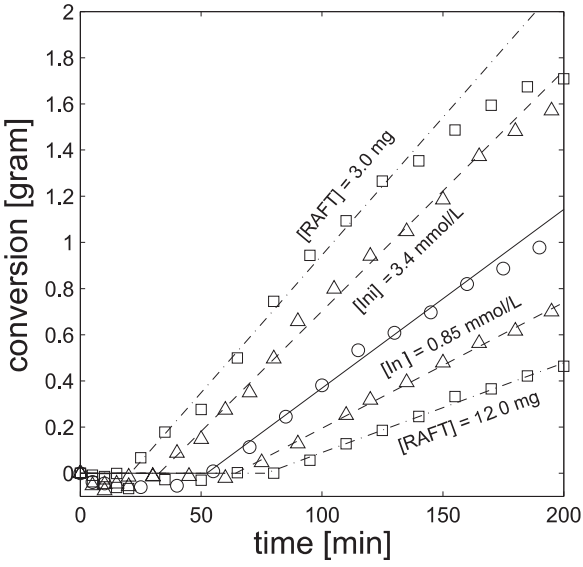

Figure 5.
Experimental conversion versus time curves for the living experiments in seeded emulsion. In the same figure, the effect of different initiator [Ini] and dormant chain [RAFT] concentration is plotted. More details in Ref. 13, Figure 2.

Table 1.
Comparison between the measured and the simulated values of inhibition time and polymerization rate at different initial concentrations of initiator and RAFT agent. For details refer to Table 5 in Ref. 13.

Run	1	2	3	4	5
Initiator [mg]	1.7	1.7	1.7	0.85	3.4
RAFT Agent [mg]	3	6	12	6	6
Inhibition Time [min] (model/experiment)	15/29	47/47	71/78	49/68	28/32
Polymerization Rate [mg/min] (model/experiment)	11.9/11.7	7.8/7.8	3.9/5.2	5.5/7.4	10.4/8.2

be concluded that in the presence of RAFT agent, all the kinetic events favor fast desorption. As a result, the reaction does not proceed, causing inhibition.

As the reaction proceeds, the amount of RAFT agent inside the particles slowly decreases and so does the frequency of exchange from N_1(long) to N_1(short). This corresponds to a reduction of the rate of desorption and, thus, to an increase in the polymerization rate, which takes place until all the RAFT agent is consumed and steady state is reached. This is depicted in Figure 7. At this point, the particles contain predominantly long dormant chains. Since upon RAFT exchange long radical chains are produced leaving unchanged the particle state, the situation is expected to be equal to that of a non-living polymerization. However, as shown in Figure 7, upon absorption of a short radical into a particle N_0, there are two pathways to change the particle state from N_1(short) to N_1(long):- the radical can either propagate, as typical of non-living reactions, or it can undergo a RAFT exchange with a long dormant chain. Notably, this exchange is typically faster than propagation and leads to the formation of short dormant chains. In other words, by radical entry a small but significant amount of short dormant chains accumulates in the particles. Once activated, these short dormant chains are producing short radicals which can promptly desorb, thus depressing the polymerization rate and causing the phenomenon of retardation. Thus concluding, both inhibition and retardation in segregated systems can be justified by accounting for the desorption of short radicals originated by the presence of short dormant chains. In other words, it is not necessary to account for the presence of radical intermediates, as in non-segregated systems, to explain inhibition and retardation.

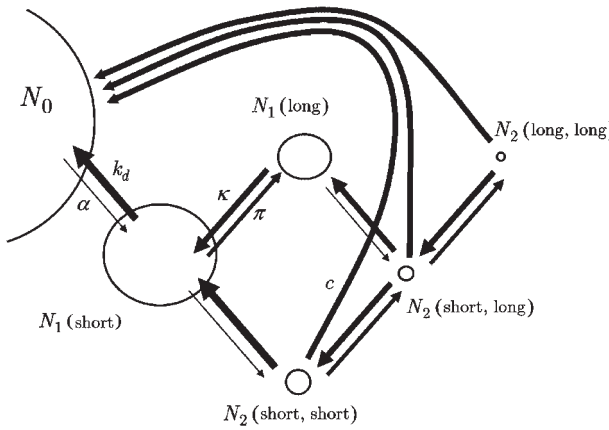

Figure 6.
Visualization of the particle population at the beginning of the living reactions (inhibition period). More details in Ref. 13, Scheme 3.

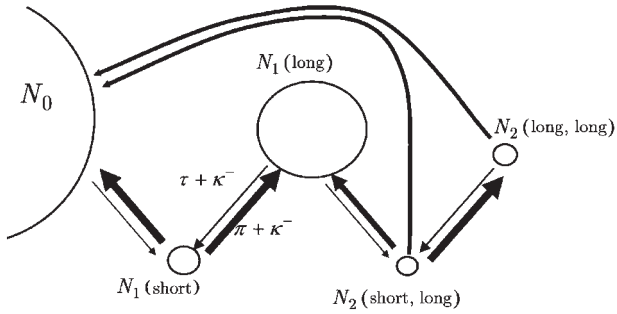

Figure 7.
Visualization of the particle population of the living reactions just after the system has reached steady state conditions (retardation). More details in Ref. 13, Scheme 4.

Gel Effect in Non-Segregated Systems

Recently, a model to evaluate the CLD and the polymerization rate in RAFT polymerizations in bulk at high conversion has been developed.[4] In the model, the presence of intermediate radicals and diffusion limitations for all involved reactions have been accounted for. Then, not only the rate constant of bimolecular termination but also that of RAFT addition are supposed to be conversion and chain-length-dependent. In particular, the kinetic rate constants of these two bimolecular reactions have been evaluated according to the following general expression:

$$\frac{1}{k_{eff}} = \frac{1}{k_0} + \frac{1}{4\pi r_{AB} \mathrm{D}_{AB} N_A} \qquad (3)$$

where k_{eff} is the effective rate constant, k_0 the kinetic rate constant of the reaction in the absence of diffusion limitations, r_{AB} and D_{AB} the radius of interaction and the mutual rate of diffusion between the chains A and B, respectively, and N_A the Avogadro's number. The diffusion coefficient, D_{AB}, is a function of both chain length of the polymers and monomer conversion. The complex resulting set of PBEs has been solved numerically with the discretization method originally proposed by Kumar and Ramkrishna.[15]

Model validation has been carried out by performing several experimental runs, operated under both living and nonliving conditions, in which the effects of the initial concentrations of initiator and RAFT agent on both the conversion and CLD as a function of time have been investigated. The diffusion limitations on the reaction rate constants have been estimated using the free volume theory of diffusion,[16] with all the involved parameters taken from independent literature sources. The only exception is represented by the chain diffusion coefficient, for which the exponential dependence on the chain length has been reduced by about 20% with respect to the original one. This change is needed to compensate for the fact that viscosity in non-living systems is smaller than that in the corresponding living systems at the same conversion, due to the fact that the polymer chains are generally shorter. The values of the reaction rate constants have also been taken from independent literature sources, with the only exception of the RAFT exchange ones, which have been fitted to the experimental data.

On the whole, the agreement of the model results with the experimental data is satisfactory. This agreement can be appreciated in Figure 8, where the comparison between the experimental data (open symbols) and the model simulation (solid curves) is shown for two sets of living reactions at different amounts of initiator (left figure) and RAFT agent (right figure), respectively. The model correctly predicts the system behavior at high conversion values, at which the effect of diffusion limitations on the reaction rate constants becomes important. In particular, it can be

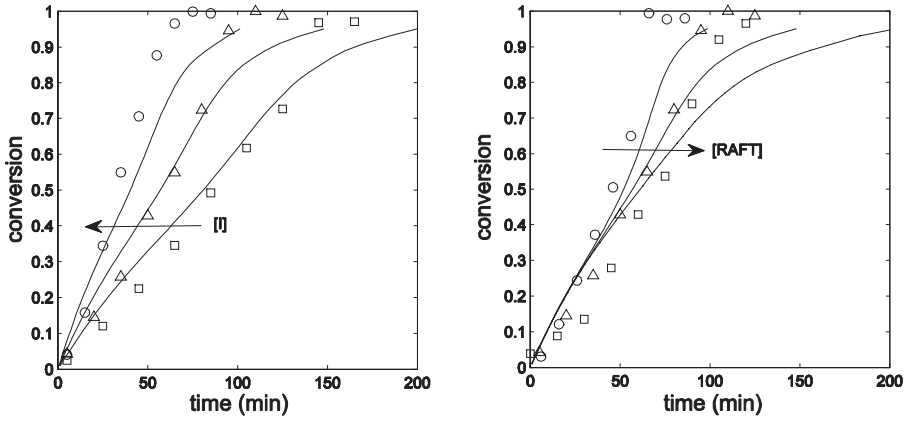

Figure 8.
Experimental conversion versus time for a living polymerization in bulk with different initial initiator concentrations (left figure) and RAFT agent concentrations (right figure). Open symbols: experimenal points; solid curves: model predictions. More details in Ref. 4(a), Figures 6 and 7.

shown that the effect of the RAFT reaction rate constants on the conversion curves is negligible, whereas the diffusion rate constant of the monomer as a function of the conversion plays a fundamental role. On the contrary, the knowledge of the rate of addition in the RAFT reaction is fundamental in the prediction of the evolution of the polymer chain distribution.

These effects have been analyzed in more detailed in a separate work.[4b] In particular, it was carried out a comparison between a model accounting for the complete CLD and a simplified model in which the different rate constants are function of the average degree of polymerization (DP), evaluated by the method of moments. Even though it was expected that for living polymerizations the results of the two models would be almost equal due to the typically small polydispersity of the CLD, it was found that the differences between the two models can actually be significant.

In order to provide a general criterion to determine a priori whether the CLD-dependent model has to be used, a critical chain length, DP_{crit}, at which the rate of the diffusion step of a bimolecular reaction equals the rate of the chemical step, i.e. where the two terms in the right hand side of Eq (3) become equal, has been defined. The so defined critical DP is shown in Figure 9 for both the bimolecular termination (dashed curve) and the RAFT addition (dash-dotted curve) reactions. In the same figure, the evolution of the average degree of polymerization of the radical chains for three different polymerizations is shown: non-living (NL), living (L) and so-called ''long''-living (LL) polymerization, where the target degree of polymerization is very large and comparable to that of the non-living case. It has been found that the two models give different results shortly after the DP of the system reaches its critical value. As far as termination rate and conversion are concerned (open circles in Figure 9), this happened below 40% conversion in all the investigated case studies.

Above this point, the conversion curves obtained with the two models differed significantly from each other, as shown in Figure 10, where the conversion plots as a function of time are reported for the three cases. Two important effects can be observed: when the critical degree of polymerization is reached (open circles), the conversion rate accelerates as a result of the diffusion limitations. At the same time, the conversion curves predicted by the complete model (dashed curves) start differing significantly from the simplified model (solid curves), where the CLD

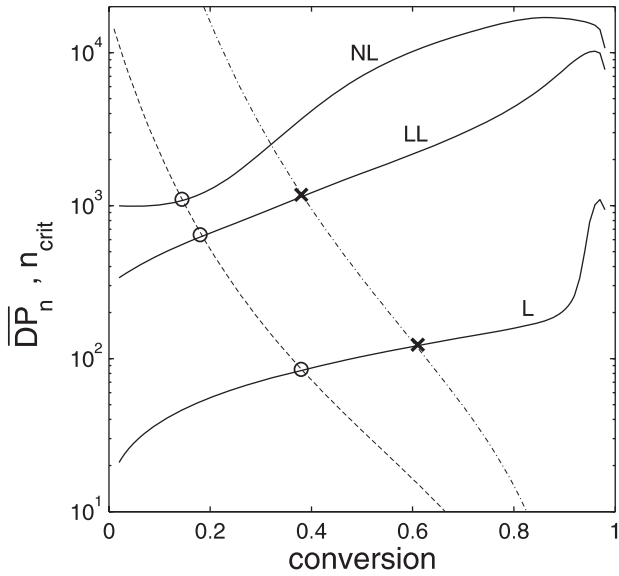

Figure 9.
Critical DP for termination (dashed curve) and RAFT addition (dash-dotted curve) as a function of conversion. Solid curves: DP for three model polymerizations. More details in Ref. 4(b), Figure 5(a).

moments only are accounted for. This difference is very pronounced even in the case of living polymerizations, in spite of the narrow chain length distribution of the radical chains observed in this case. In particular, the kinetics predicted by the simplified model is always faster than that predicted by the complete model. In fact,

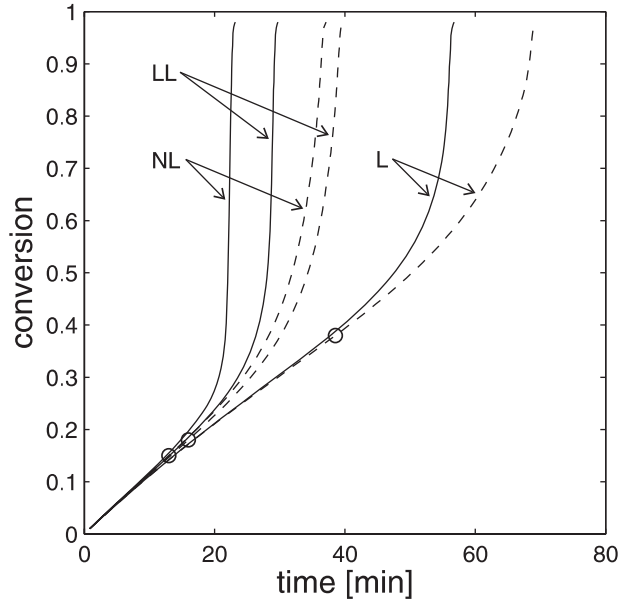

Figure 10.
Conversion curves for the model polymerizations of Figure 9. Solid curve: simplified model; dashed curves: full model; circles: conversion at which the critical DP is reached. More details in Ref. 4(b), Figure 1.

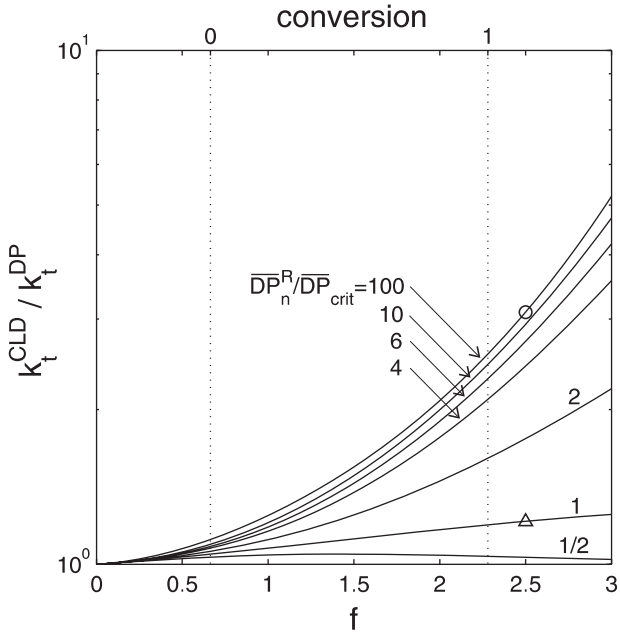

Figure 11.
Ratio between the termination rate constant computed by the complete (k_t^{CLD}) and the simplified model (k_t^{DP}) for a model distribution of radical chains with $P_d = 1.2$. See the text for the definition of f. More details in Ref. 4(b), Figure 8(a).

the role played by the short radical chains is neglected in the simplified model and the diffusion limitations are overestimated. The extent of this effect is quantified in Figure 11 for a model distribution having a relatively narrow polydispersity of the CLD equal to 1.2. In this figure, the quantity f on the abscissa is linearly proportional to conversion, as indicated by the top axis, and it represents the dependence of the diffusion coefficient of a polymer chain, D_p, upon its chain length, n ($D_p \propto n^{-f}$). It should be noticed that the value of f generally ranges between about 0.5 and 2.5 for null and full conversions, respectively (the case in Figure 11 refers to PMMA). In the same figure it can be observed that, the kinetic rate constant predicted by the complete model strongly differs from that predicted by the simplified model, especially at high conversions. This effect becomes even more pronounced when broader distributions are analyzed, for which the difference can be of several orders of magnitude. It is also worth noting that the same difference can be observed on the prediction of the CLD of the dormant chains. In Figure 12, the polydispersity predicted by the two models is compared. It

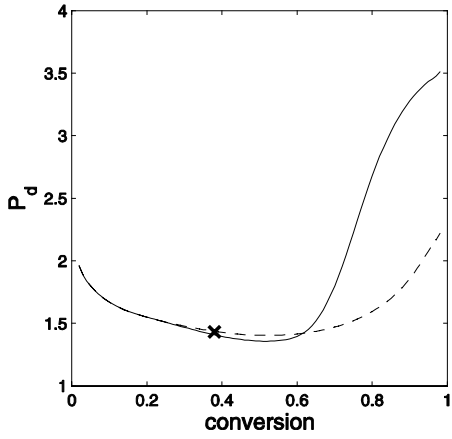

Figure 12.
Polydispersity versus conversion for the model polymerization LL of Figure 9. Solid curve: simplified model; dashed curves: complete model; cross: conversion at which the critical DP is reached. More details in Ref. 4(b), Figure 4(b).

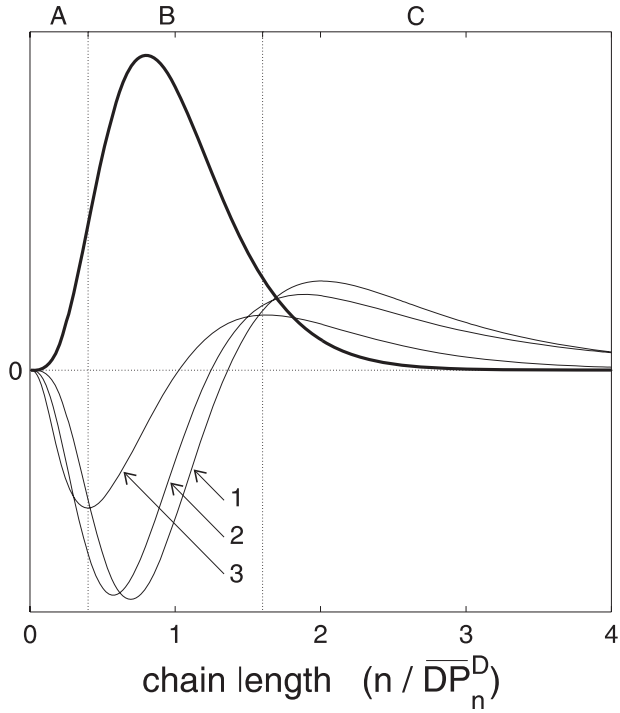

Figure 13.
Full solid curve: starting model dormant CLD; solid curves: change in the CLD (dD_n/dt) for three levels of diffusion limitations. More details in Ref. 4(b), Figure 9(c).

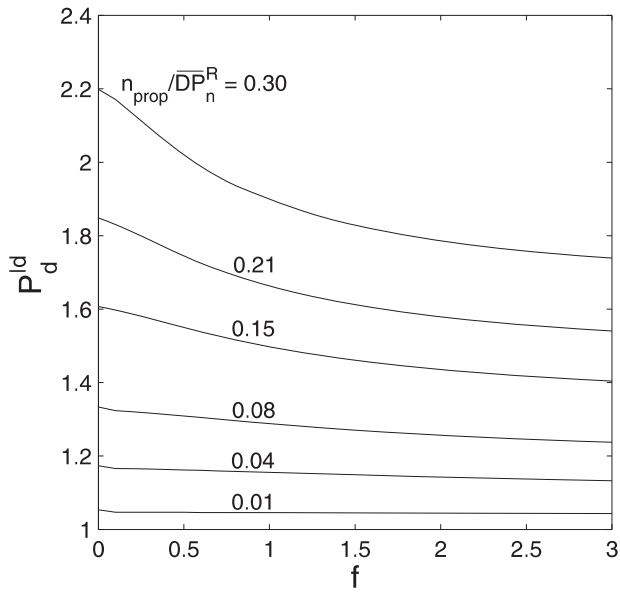

Figure 14.
Ideal polydispersity value for different intensities of the diffusion limitations (f) and different number of propagations steps per active step. See the text for the definition of f. More details in Ref. 4(b), Figure 10.

can be observed that, as soon as the critical degree of polymerization for the RAFT addition is reached (cross), the prediction of the two models starts to significantly deviate from each others.

It was also verified that diffusion limitations are favoring the production of narrower dormant chain length distributions. This effect can be observed in Figure 13, where for a model dormant CLD (bold solid curve), the change in time of the CLD has been computed for three different levels of diffusion limitations. In Case 3 (strongest diffusion limitations), the number of short dormant chains consumed is larger than in the case without diffusion limitations (Case 1), while, at the same time, the number of long dormant chains produced is smaller, thus resulting in narrower CLD. In order to quantify this effect, the concept of *ideal polydispersity* was introduced: it is the polydispersity value approached by the system when evolving under constant conditions. Two parameters are mainly affecting this value: the ratio between the average chain length and the average number of propagation steps in between two RAFT additions (n_{prop}/DP_n^R), and the intensity of diffusion limitations, quantified by the parameter f in Figure 14. It can be observed that smaller polydispersity values of the dormant CLD are obtained for both large diffusion limitations and small number of monomer additions per active period. All these important effects can be captured only if a numerical model accounting for the complete CLD is used.

Concluding Remarks

In this work, the importance of using detailed models to describe the RAFT polymerization kinetics is shown. In particular, it is shown how such models can successfully account for unexpected behaviors such as inhibition, retardation and diffusion limitations in both non-segregated (bulk) and segregated (emulsion) systems. With respect to the first two phenomena, it is important to notice that the same behavior can have very different origins. In the case of non-segregated systems, inhibition and retardation can be explained only by accounting for the complete RAFT kinetics and, in particular, by accounting for the fundamental role played by the intermediate radicals. On the other hand, it is not strictly necessary to account for these radicals to explain the same experimental evidence in segregated systems. As a matter of fact, in this case inhibition and retardation are mainly caused by radical segregation and, in particular, by desorption of radical chains caused by the activation of short dormant chains. Clearly, the same mechanisms discussed for non-segregated systems remain operative and they could partly contribute to determine the final behavior of the reaction. Future work is then needed to determine to which extent intermediate radicals can contribute to inhibition and retardation in the presence of radical segregation.

Acknowledgements: This work was financially supported by Suisse National Science Foundation (Grant No. 200020-101714).

[1] J. Chiefari, Y. K. Chong, F. Ercole, J. Krstina, J. Jeffery, T. P. T. Le, R. T. A. Mayadunne, G. F. Meijs, C. L. Moad, G. Moad, E. Rizzardo, S. H. Thang, *Macromolecules* **1998**, *31*, 5559.
[2] G. Moad, J. Chiefari, Y. K. Chong, J. Krstina, R. T. A. Mayadunne, A. Postma, E. Rizzardo, S. H. Thang, *Polym. Int.* **2000**, *49*, 993.
[3] M. Monteiro, H. de Brouwer, *Macromolecules* **2001**, *34*, 349.
[4] [4a] A. D. Peklak, A. Butté, G. Storti, M. Morbidelli, *J. Polym. Sci. Part A: Polym. Chem.* **2006**, *44*, 1071. [4b] A. D. Peklak, A. Butté, *Macromol. Theory Simul.* **2006**, *15*, 546.
[5] M. J. Monteiro, M. Hodgson, H. De Brouwer, *J. Polym. Sci. Part A: Polym. Chem.* **2000**, *38*, 3864.
[6] B. Apostolovic, F. Quattrini, A. Butté, G. Storti, M. Morbidelli, *Helv. Chim. Acta* **2006**, *89*, 1641.
[7] [7a] A. Butté, G. Storti, M. Morbidelli, *Macromolecules* **2001**, *34*, 5885; [7b] A. Butté, G. Storti, M. Morbidelli, *Macromolecules* **2000**, *33*, 3485.
[8] W. W. Smulders, C. W. Jones, F. J. Schork, *Macromolecules* **2004**, *37*, 9345.
[9] S. W. Prescott, M. J. Ballard, E. Rizzardo, R. G. Gilbert, *Macromolecules* **2002**, *35*, 5417.

[10] A. R. Wang, S. Zhu, *Macromol. Theory Simul.* **2003**, *12*, 196.
[11] H. Fischer, *Macromolecules* **1997**, *30*, 5666.
[12] A. Butté, A. D. Peklak, *Macromol. Theory. Simul.* **2006**, *15*, 285.
[13] A. D. Peklak, A. Butté, *J. Polym. Sci. Part A: Polym. Chem.* **2006**, *44*, 6144.
[14] M. Buback, P. Vana, *Macromol. Rapid Commun.* **2006**, *27*, 1299.
[15] [15a] S. Kumar, D. Ramkrishna, *Chem. Eng. Sci.* **1996**, *51*, 1311; [15b] A. Butté, G. Storti, M. Morbidelli, *Macromol. Theory Simul.* **2002**, *11*, 22.
[16] P. A. Müller, G. Storti, M. Morbidelli, *Chem. Eng. Sci.* **2005**, *60*, 377.

